CrossMark

ORIGINAL ARTICLE

Variety in excitation energy transfer processes from phycobilisomes to photosystems I and II

Yoshifumi Ueno[1] · Shimpei Aikawa[2] · Kyosuke Niwa[3] · Tomoko Abe[4] ·
Akio Murakami[1,5] · Akihiko Kondo[2] · Seiji Akimoto[1,6]

Abstract The light-harvesting antennas of oxygenic photosynthetic organisms capture light energy and transfer it to the reaction centers of their photosystems. The light-harvesting antennas of cyanobacteria and red algae, called phycobilisomes (PBSs), supply light energy to both photosystem I (PSI) and photosystem II (PSII). However, the excitation energy transfer processes from PBS to PSI and PSII are not understood in detail. In the present study, the energy transfer processes from PBS to PSs in various cyanobacteria and red algae were examined in vivo by selectively exciting their PSs or PBSs, and measuring the resulting picosecond to nanosecond time-resolved fluorescences. By observing the delayed fluorescence spectrum of PBS-selective excitation in *Arthrospira platensis*, we demonstrated that energy transfer from PBS to PSI via PSII (PBS→PSII→PSI transfer) occurs even for PSI trimers. The contribution of PBS→PSII→PSI transfer was species dependent, being largest in the wild-type of red alga *Pyropia yezoensis* (formerly *Porphyra yezoensis*) and smallest in *Synechococcus* sp. PCC 7002. Comparing the time-resolved fluorescence after PSs- and PBS-selective excitation, we revealed that light energy flows from CP43 to CP47 by energy transfer between the neighboring PSII monomers in PBS–PSII supercomplexes. We also suggest two pathways of energy transfer: direct energy transfer from PBS to PSI (PBS→PSI transfer) and indirect transfer through PSII (PBS→PSII→PSI transfer). We also infer that PBS→PSI transfer conveys light energy to a lower-energy red chlorophyll than PBS→PSII→PSI transfer.

Keywords Energy transfer · Phycobilisome · Photosystem · Delayed fluorescence · Cyanobacteria · Red algae

Abbreviations
APC   Allophycocyanin
Chl   Chlorophyll
GM   Green mutant
PBS   Phycobilisome
PC   Phycocyanin
PE   Phycoerythrin
PS   Photosystem
TRFS   Time-resolved fluorescence spectrum (spectra)
WT   Wild-type

✉ Seiji Akimoto
akimoto@hawk.kobe-u.ac.jp

1 Graduate School of Science, Kobe University,
Kobe 657-8501, Japan

2 Graduate School of Engineering, Kobe University,
Kobe 657-8501, Japan

3 Fisheries Technology Institute, Hyogo Prefectural
Technology Center for Agriculture, Forestry and Fisheries,
Akashi, Hyogo 674-0093, Japan

4 RIKEN Nishina Center for Accelerator-Based Science,
Wako, Saitama 351-0198, Japan

5 Kobe University Research Center for Inland Seas,
Awaji 656-2401, Japan

6 Molecular Photoscience Research Center, Kobe University,
Kobe 657-8501, Japan

Introduction

The unique light-harvesting antennas of oxygenic photosynthetic organisms contain pigments such as chlorophyll (Chl), carotenoid, and phycobilin. The light energy captured by these antennas is transferred to the reaction centers of the photosystems (PSs), where photochemical reactions

proceed. A photochemical reaction in the reaction center induces electron flow from water to NADP$^+$, generating a proton-motive force across the thylakoid membranes for ATP synthesis. Efficient oxygenic photosynthesis relies on the proper control of energy transfer from the light-harvesting antennas to both PSs (PSI and PSII).

Cyanobacteria and red algae possess a large light-harvesting antenna called phycobilisome (PBS) on their thylakoid membrane surfaces (Gantt 1981). PBS comprises an allophycocyanin (APC) core surrounded by phycocyanin (PC)-containing rods, which absorb visible light. The PC may be pure or combined with phycoerythrin (PE) (Gantt 1981; Adir 2005). Although the morphology of PBS differs between cyanobacteria and red algae (Arteni et al. 2008, 2009), the energy transfer efficiency of PBS in both taxa approaches 100% (Glazer 1984). PBS is generally known as the light-harvesting antenna of PSII. The energy transfer pathways from PBS to PSII have been investigated in fluorescence measurements of CP43-deficient and CP47-deficient mutants of *Synechocystis* (Bittersmann and Vermaas 1991; Shimada et al. 2008). However, as neither of these mutants transfer energy from PBS to PSII (PBS→PSII transfer) (Bittersmann and Vermaas 1991; Shimada et al. 2008), the details of the energy transfer remain unclear. PBS can supply light energy to PSI under intense light conditions, or under light that excites PSII (Mullineaux 2008). Energy transfer from PBS to PSI is thought to occur by two pathways: direct energy transfer from PBS to PSI (PBS→PSI transfer) (Allen et al. 1985) or indirect energy transfer from PBS to PSI via PSII (spillover after PBS→PSII transfer, i.e., PBS→PSII→PSI transfer) (Murata 1969). The occurrences of both transfers have been studied by various methods such as steady-state fluorescence spectra at 77 K (Bruce et al. 1989), photooxidation rates of P700 (Ley and Butler 1977), electron microscopy (Olive et al. 1997), and fluorescence recovery after photobleaching (Mullineaux et al. 1997). However, the energy transfer processes from PBS to PSI remained incompletely understood.

Recently, we demonstrated the existence of PSII→PSI transfer by measuring the delayed fluorescence (Yokono et al. 2011), which originates from charge recombination at the PSII reaction center (Mimuro et al. 2007). More recently, we measured the delayed fluorescence spectra under PBS-selective excitation, and confirmed the occurrence of PBS→PSII→PSI transfer in vivo in cyanobacteria; *Synecocystis* sp. PCC 6803 (hereafter referred to as *Synechocystis*), *Synechococcus* sp. PCC 7002 (*Synechococcus*), and the red alga *Cyanidioschyzon merolae* (Ueno et al. 2016). Such interactions were never observed in isolated PBS–PSII–PSI megacomplexes (Liu et al. 2013). However, 5–7 ns after 400-nm excitation of cyanobacterial cells, we observed shorter PSI peak wavelength in the

delayed fluorescence than in the time-resolved fluorescence spectrum (TRFS) (Akimoto et al. 2014). Therefore, the PBS→PSI and PBS→PSII→PSI pathways may transfer light energy to PSI Chls with different energy levels. In the present study, we examined the energy transfer processes from PBS to PSs in various cyanobacterial and red algal cells. To this end, we supplemented our previous samples with the cyanobacterium *Arthrospira platensis*, and a wild-type (WT) and a green mutant (GM) of the red alga *Pyropia yezoensis*. *A. platensis* exhibits two peaks around 730 and 760 nm in the PSI fluorescence region; the latter is attributed to PSI trimers (Shubin et al. 1993). Unlike the PBS of *C. merolae*, the PBS of *P. yezoensis* contains APC, PC, and PE, of which the PE contents are reduced in the mutant (Niwa et al. 2009). We also selectively excited the PSs or PBS of the above organisms, and measured and compared their resulting time-resolved fluorescences at 77 K. Fluorescence peaks from the different components are better-resolved at 77 K than at room temperatures since there is less thermal energy to help excitons on long-wavelength pigments escape at 77 K.

Materials and methods

Cultivation conditions

Cyanobacteria *Synechocystis* and *Synechococcus*, and red alga *C. merolae* 10D were grown under previously described conditions (Ueno et al. 2016). The growth conditions of the cyanobacterium *A. platensis* NIES39 are also described elsewhere (Akimoto et al. 2012). In the present study, we employed the WT strain (HG-5) and the GM strain (IBY-G3) of *Pyropia yezoensis*. The WT was a pure line of cultivated *P. yezoensis* isolated by the method of Niwa et al. (2004). The GM was isolated from a green-cell cluster of the WT blade mutated by carbon-ion beam (50 Gy, 23 keV/μm) irradiation as described in Niwa et al. (2009). Gametophytic blades of WT and GM were laboratory cultured under the conditions described in Niwa et al. (2009).

Measurements and analyses

Steady-state fluorescence spectra were measured by a spectrofluorometer (JASCO FP-6600/PMU-183) operated at 77 K (Ueno et al. 2015). The excitation wavelength was set to 408 nm (exciting PSs) or 635 nm (exciting PBS). As the steady-state fluorescence spectra of *P. yezoensis*, we used the time-integrated fluorescence spectra constructed by integrating the TRFS. The TRFS were measured by a time-correlated single-photon counting system at 77 K (Akimoto et al. 2012), with the excitation wavelength set to 408 or 633 nm

(exciting PSs or PBS, respectively). The repetition rate of the pulse train was 5 MHz. To accurately evaluate the delayed fluorescence, we set the time interval of data acquisition to 24.4 ps/channel (total time window = 100 ns). The fluorescence kinetics were measured at 1-nm intervals (675–750 or 675–775 nm in the case of *A. platensis*). To accurately evaluate the fluorescence kinetics, we also measured the fluorescence rise and decay curves up to 10 ns (2.44 ps/channel × 4096 channels), which covers the delayed fluorescence peaks of PSI and PSII. The fluorescence rise and decay curves at different detection wavelengths were obtained at different excitation wavelengths, and globally fitted by sums of exponentials with common time constants as follows:

$$F(t, \lambda) = \sum_{n=1}^{7} A_n(\lambda) \exp\left(-\frac{t}{\tau_n}\right). \tag{1}$$

Here, $A_n(\lambda)$ is the amplitude at the detection wavelength λ and τ_n is the time constant.

For both steady-state and time-resolved fluorescence measurements, we obtained homogenous ice at 77 K by adding polyethylene glycol (average molecular weight 3350, final concentration 15% (w/v), Sigma-Aldrich, St Louis, MO, USA) to the sample solutions (Mimuro et al. 1989). Prior to measurements, all samples were dark adapted for ~20 min.

Results

Steady-state fluorescence spectra

Figure 1 shows the steady-state fluorescence spectra of various cyanobacteria and red algae after selective excitation of PSs and PBS. The spectra are divided into two

Fig. 1 Steady-state fluorescence spectra of *Synechocystis* sp. PCC 6803 (**a**), *Synechococcus* sp. PCC 7002 (**b**), *Arthrospira platensis* (**c**), *Cyanidioschyzon merolae* (**d**), and *Pyropia yezoensis* wild-type (**e**) and green mutant (**f**) at 77 K. Each spectrum is normalized by its maximum intensity. *Blue* and *red lines* indicate PSs- and PBS-selective excitation, respectively. The *Pyropia yezoensis* spectra are the time-integrated fluorescence spectra. *Labels in each spectrum* indicate the PSI fluorescence peak position
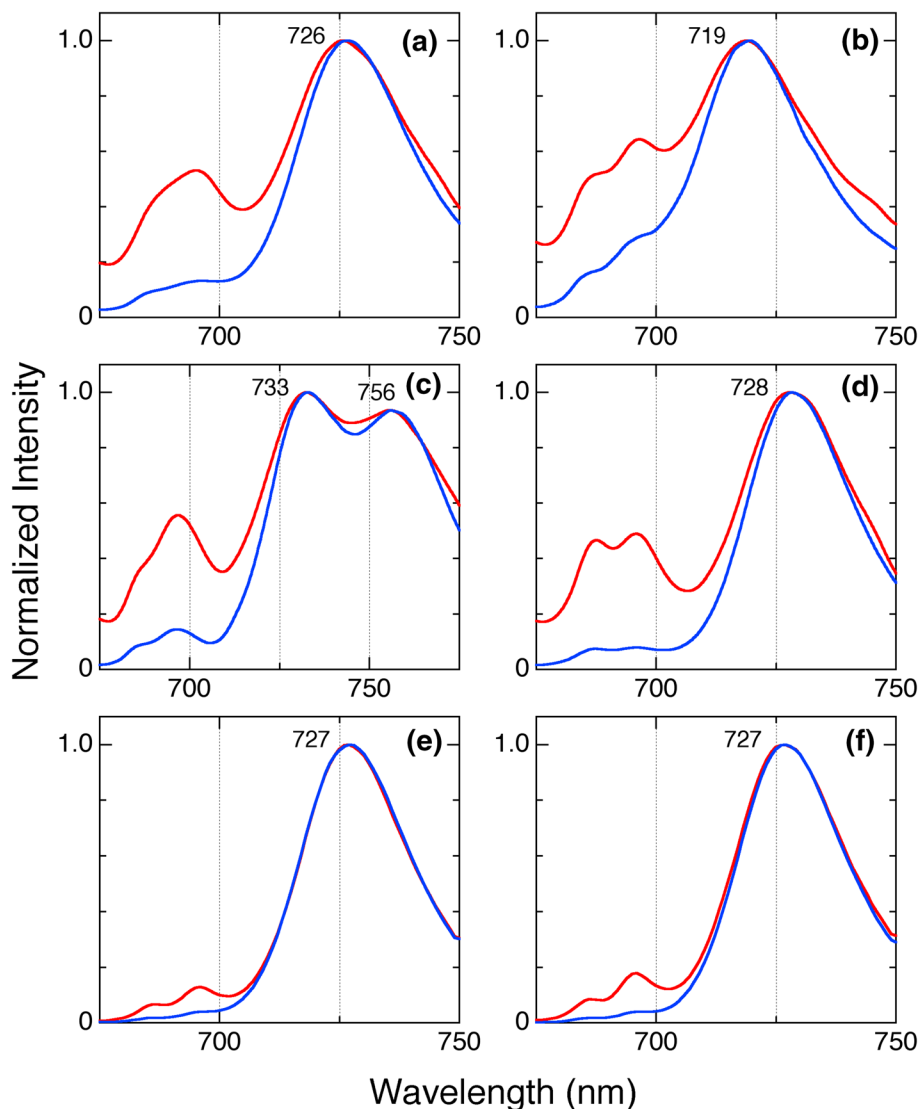
fluorescence regions: PSII (675–700 nm) and PSI (longer than 700 nm). In the PSII fluorescence region, the peaks around 685 and 695 nm are assigned to CP43 and CP47, respectively (Murata and Satoh 1986). The PSI fluorescence region generally exhibits a single peak; the exception is *A. platensis*, which yields two fluorescence bands around 730 and 760 nm. The latter band derives from PSI trimers (Shubin et al. 1993). Although PBS-selective excitation induces detectable PSI fluorescence, it yields a lower fluorescence intensity ratio of PSI to PSII than PSs-selective excitation. The two peaks in the PSI fluorescence region of the *A. platensis* spectrum indicate that in this species, energy is transferred from PBS to both monomers and trimers of PSI.

Time-resolved fluorescence spectra

To examine the energy transfer processes from PBS to PSI and PSII, we measured the TRFS after excitation at 408 or

633 nm. Figure 2 shows TRFS of the various cyanobacteria and red algae after excitation at both wavelengths. The peak assignments are essentially those of the steady-state fluorescence spectra. The 408-nm excitation is mainly absorbed by PSs, indicating energy transfer between and within PSI and PSII. Immediately after the PSs-selective excitation (blue lines in Fig. 2), two bands are observed, but the PSI band is more intense than the PSII band. The CP47 fluorescence band in the PSII fluorescence region clearly persists over time, whereas the PSI fluorescence band shifts to longer wavelengths, reaching its longest wavelength band after 3.5–4.0 and 9.4–11 ns in cyanobacteria and red algae, respectively. In *A. platensis*, the fluorescence intensity around 760 nm increases after 610–730 ps, forming a clear band that persists over time. The TRFS at 47–76 ns are the delayed fluorescence spectra derived from charge recombination at the PSII reaction center (Mimuro et al. 2007). In previous studies of isolated PSI and light-harvesting antennas, no delayed fluorescence was observed in the time
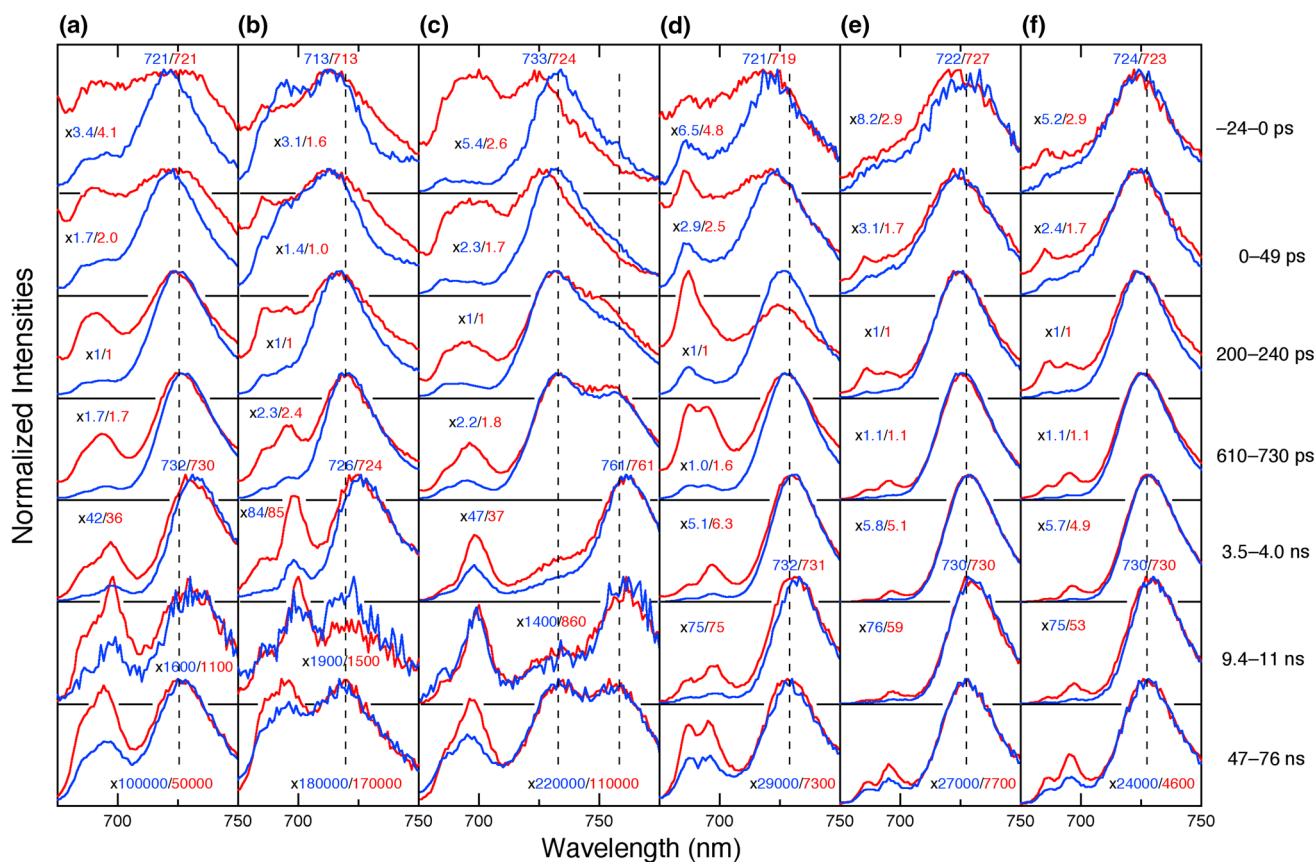

Fig. 2 Time-resolved fluorescence spectra of *Synechocystis* sp. PCC 6803 (**a**), *Synechococcus* sp. PCC 7002 (**b**), *Arthrospira platensis* (**c**), *Cyanidioschyzon merolae* (**d**), and *Pyropia yezoensis* wild-type (**e**) and green mutant (**f**) at 77 K. The excitation wavelength was 408 nm (*blue lines*) or 633 nm (*red lines*). Zero time corresponds to the time of maximum intensity of the excitation laser pulse. Each spectrum is normalized by its maximum intensity. *Numbers in each panel* indicate the magnification factors relative to the most intense spectrum. *Vertical lines* indicate the delayed fluorescence peaks of PSI. The PSI fluorescence peak positions are displayed in TRFS at −24–0 ps, and 3.5–4.0 and 9.4–11 ns in cyanobacteria and red algae, respectively

region of the present study (Mimuro et al. 2010; Yokono et al. 2015a). Therefore, in the absence of PSII→PSI transfer, the delayed fluorescence is contributed by PSII alone. Conversely, PSII→PSI transfer will manifest as delayed fluorescence in the PSI fluorescence region (Yokono et al. 2011). The observed PSI fluorescence band in the delayed fluorescence spectra indicates that PSII→PSI transfer occurs in our algae.

The 633-nm laser excitation is mainly absorbed by PBS. At this excitation wavelength, the TRFS reflect the energy transfer from PBS to PSs and subsequent energy transfer between and within PSI and PSII. Immediately after the PBS-selective excitation (red lines in Fig. 2), PSI and PSII bands are detected, and CP43 fluorescence appears in the PSII fluorescence region of all spectra except that of *A. platensis*. The fluorescence intensities of CP43 and CP47 are comparable in *A. platensis*. The CP47 fluorescence band is detectable after 200 ps in *Synechocystis, Synechococcus*, and *P. yezoensis*, whereas in *C. merolae*, the PSII fluorescence overtakes the PSI fluorescence after 200 ps and the CP47 fluorescence band is clearly observed after 610 ps. Meanwhile, the PSI fluorescence band is redshifted over time, and its longest wavelength band coincides with the wavelength of PSs-selective excitation. The TRFS at 47–76 ns after PBS-selective excitation are also delayed fluorescence spectra (Mimuro et al. 2007). Previously, we identified PBS→PSII→PSI transfer in *Synechocystis, Synechococcus*, and *C. merolae* by observing PSI fluorescence in their delayed fluorescence spectra after PBS-selective excitation (Ueno et al. 2016). Here, we also recognize PBS→PSII→PSI transfer in *A. platensis* and *P. yezoensis*. The delayed fluorescence spectra in the PSI fluorescence region after PBS-selective excitation peak at the wavelength of PSs-selective excitation, indicating that the spillover pathway is conserved regardless of connection or disconnection of PBS and PSII.

Immediately after the PBS-selective excitation, *Synechocystis, Synechococcus*, and *C. merolae* exhibit a broader band in the PSI fluorescence region than under PSs-selective excitation. The peak in the *A. platensis* and *P. yezoensis* WT spectra appears at shorter wavelengths than in the PSs-selective excitation, whereas the *P. yezoensis* GM spectrum exhibit no clear differences. In addition, the fluorescence intensity ratio of CP47 to CP43 in the delayed fluorescence is higher under PBS-selective excitation than under PSs-selective excitation, except in *C. merolae*.

Fluorescence rise and decay kinetics

To evaluate the fluorescence kinetics in PSI and PSII, we globally analyzed the measured fluorescence rise and decay curves at different detection wavelengths for different excitation wavelengths. The curves were fitted by seven exponentials with common time constants. The results are listed in Table 1. After PBS-selective excitation, the two shortest-lived components (τ_1 and τ_2) typically took negative amplitudes, indicating that CP43, CP47, and PSI receive energy from PBS in both fast phase (τ_1) and slow phase (τ_2). The fast-phase contributions are negligible only in *A. platensis*, and fast-phase energy transfer to CP43 is absent in *C. merolae*. However, the time constant of the slow phase was shorter in *C. merolae* than in *P. yezoensis*. Therefore, compared with *P. yezoensis*, the efficiency of PBS→CP43 transfer in *C. merolae* is moderately large. *Synechococcus* alone exhibits a fast phase in PBS→CP47 transfer. Fast energy transfer to PSI operates only in *C. merolae* and *P. yezoensis* GM. The τ_4 and τ_5 components represent the fluorescence lifetimes of red Chls with different energy levels. The τ_5 component probably originates from the red Chl with lowest energy, because its PSI fluorescence peak was redshifted over time. The τ_4 and τ_5 lifetimes differ between cyanobacteria (~500–750 ps and ~1.5 ns, respectively) and red algae (~1 and ~2 ns, respectively). These differences may reflect the environmental differences around red Chl in the two organisms.

Discussion

Energy transfer from PBS to PSII

Immediately after PBS-selective excitation, differences between the CP43 and CP47 bands were observed. The spectra of all algae except *A. platensis* displayed a CP43 fluorescence band, whereas the fluorescence intensities of CP43 and CP47 were comparable in *A. platensis*. This result confirms PBS→CP43 transfer as the main pathway in *Syenchocystis, Synechococcus, C. merolae*, and *P. yezoensis*. In *A. platensis*, the energy transfer was almost equally split between PBS→CP43 and PBS→CP47. The intensity of the CP47 fluorescence band of *A. platensis* increased over time, as reported for the filamentous cyanobacterium *Halomicronema hongdechloris* (Tomo et al. 2014).

Delayed PSII fluorescence originates from PSII complexes that do not connect with PSI (i.e., PSII complexes and PBS–PSII supercomplexes) (Yokono et al. 2011). The information from delayed florescence spectra can be altered by changing the excitation wavelength. Under PSs-selective excitation, the delayed florescence spectra characterize the PSII complexes and PBS–PSII supercomplexes, whereas under PBS-selective excitation, they mainly characterize the PBS–PSII supercomplexes. Apart from *C. merolae*, the delayed fluorescence intensity at CP47 to CP43 is larger under PBS-selective excitation (c.f. PSs-selective excitation) (TRFS at 47–76 ns, Fig. 2). In their electron microscopy studies, Mörschel and

Table 1 Time constants of the 1st to 5th components, and their amplitudes, after global fitting of the fluorescence rise and decay curves after 408- or 633-nm excitation (Ex 408 or Ex 633, respectively) of *Synechocystis* sp. PCC 6803, *Synechococcus* sp. PCC 7002, *Arthrospira platensis*, *Cyanidioschyzon merolae*, and *Pyropia yezoensis* wild-type (WT) and green mutant (GM)

	Wavelength	Assignment	$\tau_1 = 15$ ps	$\tau_2 = 50$ ps	$\tau_3 = 250$ ps	$\tau_4 = 0.75$ ns	$\tau_5 = 1.4$ ns
Synechocystis							
Ex 408	686 nm	CP43	0.654	0.055	0.259	0.019	0.013
	694 nm	CP47	0.753	0.014	0.159	0.061	0.014
	724 nm	PSI	–	−0.396	0.534	0.405	0.060
Ex 633	686 nm	CP43	−0.256	−0.356	0.863	0.077	0.059
	694 nm	CP47	−0.006	−0.125	0.714	0.213	0.071
	724 nm	PSI	−0.216	−0.768	0.530	0.358	0.111
	Wavelength	Assignment	$\tau_1 = 15$ ps	$\tau_2 = 45$ ps	$\tau_3 = 160$ ps	$\tau_4 = 0.62$ ns	$\tau_5 = 1.4$ ns
Synechococcus							
Ex 408	686 nm	CP43	0.404	0.284	0.284	0.025	0.003
	694 nm	CP47	0.340	0.462	0.153	0.037	0.008
	720 nm	PSI	–	−0.386	0.597	0.376	0.026
Ex 633	686 nm	CP43	−0.475	−0.135	0.938	0.042	0.020
	694 nm	CP47	−0.598	0.045	0.810	0.111	0.034
	720 nm	PSI	−0.039	−0.178	0.674	0.280	0.046
	Wavelength	Assignment	$\tau_1 \leq 10$ ps	$\tau_2 = 90$ ps	$\tau_3 = 150$ ps	$\tau_4 = 0.52$ ns	$\tau_5 = 1.5$ ns
A. platensis							
Ex 408	686 nm	CP43	0.130	0.300	0.271	0.285	0.013
	694 nm	CP47	0.693	0.039	–	0.227	0.039
	730 nm	PSI	−0.006	−0.680	0.728	0.266	0.006
	760 nm	PSI	−0.020	−0.454	0.152	0.619	0.227
Ex 633	686 nm	CP43	−0.024	−0.703	0.786	0.193	0.020
	694 nm	CP47	–	−0.396	0.375	0.502	0.120
	730 nm	PSI	–	−0.612	0.327	0.635	0.036
	760 nm	PSI	–	−0.685	–	0.649	0.345
	Wavelength	Assignment	$\tau_1 = 15$ ps	$\tau_2 = 50$ ps	$\tau_3 = 190$ ps	$\tau_4 = 1.1$ ns	$\tau_5 = 2.2$ ns
C. merolae							
Ex 408	686 nm	CP43	0.136	–	0.727	0.125	0.008
	694 nm	CP47	0.700	–	0.047	0.239	0.009
	726 nm	PSI	–	−0.471	–	0.481	0.514
Ex 633	686 nm	CP43	–	−0.742	0.826	0.168	0.003
	694 nm	CP47	−0.066	−0.599	0.477	0.453	0.064
	726 nm	PSI	−0.473	−0.494	0.381	–	0.607
	Wavelength	Assignment	$\tau_1 = 15$ ps	$\tau_2 = 60$ ps	$\tau_3 = 190$ ps	$\tau_4 = 1.0$ ns	$\tau_5 = 2.3$ ns
P. yezoensis WT							
Ex 408	686 nm	CP43	0.155	0.003	0.740	0.091	0.004
	694 nm	CP47	0.291	0.381	0.140	0.158	0.023
	725 nm	PSI	−0.094	−0.754	0.081	0.515	0.399
Ex 633	686 nm	CP43	−0.360	−0.631	0.934	0.055	0.009
	694 nm	CP47	–	−0.117	0.499	0.426	0.066
	725 nm	PSI	−0.041	−0.337	0.082	0.358	0.547

Table 1 (continued)

	Wavelength	Assignment	$\tau_1 = 25$ ps	$\tau_2 = 65$ ps	$\tau_3 = 220$ ps	$\tau_4 = 1.1$ ns	$\tau_5 = 2.3$ ns
P. yezoensis GM							
Ex 408	686 nm	CP43	0.381	0.045	0.497	0.070	0.004
	694 nm	CP47	0.680	–	0.152	0.137	0.027
	725 nm	PSI	−0.088	−0.633	–	0.561	0.436
Ex 633	686 nm	CP43	−0.818	−0.163	0.901	0.082	0.013
	694 nm	CP47	–	−0.070	0.367	0.533	0.085
	725 nm	PSI	−0.128	−0.087	0.073	0.280	0.628

–: not detectable

Sum of the positive amplitudes (including those of the 6th and 7th components) at each fluorescence wavelength is normalized to unity. The time constants of the 6th and 7th components are 4.7–6.2 and 16–26 ns, respectively

Schatz (1987) reported that PBS mainly combines with the PSII dimer. Strong interaction between the PSII monomers induces energy transfer from CP43 to its neighboring CP47 (Yokono et al. 2012). Our study reveals that light energy flows from CP43 to CP47 by energy transfer between the neighboring PSII monomers in intact PBS–PSII supercomplexes. Energy transfer to CP47 might relate to spillover, as suggested previously (McConnell et al. 2002). In contrast to other algae, the CP43 and CP47 of *C. merolae* fluoresced with almost identical intensity under PBS-selective excitation. Although the CP43 fluorescence in *C. merolae* is large in the early time region (TRFS at 200–240 ps, Fig. 2), energy transfer between neighboring PSII monomers functions in this red alga.

At 77 K, excitation energy is transferred from higher-energy pigments to lower-energy pigments, and fluorescence is mainly emitted from terminal energy traps. On the other hand, up-hill energy transfer occurs at physiological temperatures. Therefore, energy is shared among CP43, CP47, and the reaction center via energy transfer between neighboring PSII monomers. Interactions between the PSII monomers in the PSII dimer change depend not only on species but also on pH (Yokono et al. 2015b). Therefore, by controlling the interactions between the PSII monomers in their PSII dimers, the algae might effectively perform charge separation at their reaction centers.

Energy transfer from PBS to PSI

Energy transfer from PBS to PSI occurs by two pathways: PBS→PSI transfer (Allen et al. 1985) and PBS→PSII→PSI transfer (Murata 1969). The delayed fluorescence spectra of all algae (TRFS at 47–76 ns, Fig. 2) exhibit a clear PSI fluorescence band, indicating that PBS→PSII→PSI transfer occurs in all of the investigated algae. Under PBS-selective excitation, the fluorescence intensity ratio of PSI to PSII in the delayed fluorescence reflects the contribution of the PBS→PSII→PSI transfer. The larger the intensity, the higher the contribution (Yokono et al. 2011). The fluorescence intensity ratios of PSI to PSII in the delayed fluorescence after PSs- and PBS-selective excitations are listed in Table 2. Under PBS-selective excitation, the contribution of PBS→PSII→PSI transfer was largest in *P. yezoensis* WT and smallest in *Synechococcus*. The intensity ratios of PSI to PSII in the delayed fluorescence were almost halved in the PBS-selective excitation, relative to the PSs-selective excitation. The sole exception was *Synechococcus*, for which the delayed fluorescence intensities were almost identical under both excitations (Table 2). This suggests

Table 2 Fluorescence intensity ratio of PSI to PSII in the delayed fluorescence spectra (TRFS at 47–76 ns) of *Synechocystis* sp. PCC 6803, *Synechococcus* sp. PCC 7002, *Arthrospira platensis, Cyanidi-oschyzon merolae,* and *Pyropia yezoensis* wild-type and green mutant excited at 408 or 633 nm (Ex 408 or Ex 633, respectively)

	Synechocystis	*Synechococcus*	*A. platensis*	*C. merolae*	*P. yezoensis* WT	*P. yezoensis* GM
Ex 408	1.67	0.77	2.24	1.57	4.24	3.86
Ex 633	0.85	0.69	1.19	0.72	1.96	1.81

The PSII fluorescence intensity was determined by averaging the fluorescence intensities of the CP43 and CP47 bands. The PSI intensity of the *A. platensis* spectrum was averaged from the fluorescence intensities of the two bands at 730 and 760 nm. The PSI fluorescence intensity was determined by subtracting $0.2 \times$ PSII fluorescence intensity from the observed fluorescence intensity at the PSI peak (Yokono et al. 2015a). Moreover, the PSI and PSII fluorescence intensities were divided by their corresponding mean fluorescence lifetimes (Yokono et al. 2011)

that most of the PSII–PSI supercomplexes connect with PBS in *Synechococcus*.

The relative amplitude of the τ_5 component was higher under PBS-selective excitation than under PSs-selective excitation (Table 1), indicating that energy is transferred from PBS to low-energy red Chls. In the cyanobacteria *Synechocystis* and *Synechococcus*, the PSI peak is clearly blueshifted as the TRFS advances from 3.5 to 4.0 ns to delayed fluorescence (Fig. 2). Similarly, the red algae *C. merolae* and *P. yezoensis* exhibit a slight blueshift in the PSI peak wavelength as the TRFS progresses from 9.4 to 11 ns to delayed fluorescence (Fig. 2). These results suggest that PBS→PSI transfer supplies light energy to lower-energy red Chls than PBS→PSII→PSI transfer in *Synechocystis, Synechococcus, C. merolae*, and *P. yezoensis*. PSI exists as a monomer in red algae (Gardian et al. 2007), but can be monomeric or trimeric in cyanobacteria (Kruip et al. 1994). Under PBS-selective excitation, the delayed fluorescence spectrum of *A. platensis* showed two peaks around 730 and 760 nm (TRFS at 47–76 ns, Fig. 2). The peak around 760 nm is unique to PSI trimers (Shubin et al. 1993), implying that PBS–PSII–PSI megacomplexes contain both monomeric and trimeric PSI in vivo.

Immediately after the PBS-selective excitation, the *Synechocystis* and *Synechococcus* spectra showed a broad, intense PSI fluorescence band at the longer wavelength side. This suggests that the PBS→PSI transfer delivers light to low-energy red Chls. Conversely, *C. merolae* exhibits a broad enhanced band at the shorter wavelength side, whereas *A. platensis* shows a blueshifted peak. These results suggest that light flows from PBS to higher-energy red Chls in these organisms. The clear PSI band in the spectrum of *P. yezoensis* indicates a large contribution by PSII→PSI transfer (Table 2). However, under PBS-selective excitation, the peak PSI shifts to shorter wavelengths in WT, but not in GM. Beyond 200 ps, the TRFS of WT and GM peak at similar wavelengths. PE level is considerably lower in the GM than in the WT (Niwa et al. 2009). Therefore, the PE contents affect the energy transfer pathways from PBS (APC) to PSI, but not the energy transfers within the PSI.

Summary

We examined the excitation energy transfer processes from PBS to PSs in cyanobacteria (*Synechocystis, Synechococcus*, and *A. platensis*) and red algae (*C. merolae* and *P. yezoensis*). Observing the delayed fluorescence spectra after PBS-selective excitation, we confirmed PBS→PSII→PSI energy transfer in all of the examined algae (TRFS at 47–76 ns, Fig. 2). We also demonstrated that the PBS–PSII–PSI megacomplexes of cyanobacteria contain both monomeric and trimeric PSI, both of which undergo PBS→PSII→PSI transfer (Fig. 2). The contribution of PBS→PSII→PSI transfer was largest in *P. yezoensis* WT and smallest in *Synechococcus* (Table 2). We suggest that in vivo, the PBS→PSI pathway transfers light energy to lower-energy red Chls than the PBS→PSII→PSI pathway (Fig. 2; Table 1). Comparing the time-resolved fluorescences after PSs- and PBS-selective excitation, we revealed that CP43→CP47 energy transfer occurs between neighboring PSII monomers in the PBS–PSII supercomplexes (TRFS at 47–76 ns, Fig. 2). We also suggest that most of the PSII–PSI supercomplexes connect with PBS in *Synechococcus* (Table 2).

References

Adir N (2005) Elucidation of the molecular structures of components of the phycobilisome: reconstructing a giant. Photosynth Res 85:15–32

Akimoto S, Yokono M, Hamada F, Teshigahara A, Aikawa S, Kondo A (2012) Adaptation of light-harvesting systems of *Arthrospira platensis* to light conditions, probed by time-resolved fluorescence spectroscopy. Biochim Biophys Acta 1817:1483–1489

Akimoto S, Yokono M, Yokono E, Aikawa S, Kondo A (2014) Short-term light adaptation of a cyanobacterium *Synechocystis* sp. PCC 6803, probed by time-resolved fluorescence spectroscopy. Plant Physiol Biochem 81:149–154

Allen JF, Sanders CE, Holmes NG (1985) Correlation of membrane protein phosphorylation with excitation energy distribution in the cyanobacterium *Synechococcus* 6301. FEBS Lett 193:271–275

Arteni AA, Liu LN, Aartsma TJ, Zhang YZ, Zhou BC, Boekema EJ (2008) Structure and organization of phycobilisomes on membranes of the red alga *Porphyridium cruentum*. Photosynth Res 95:169–174

Arteni AA, Ajlani G, Boekema EJ (2009) Structural organisation of phycobilisomes from *Synechocystis* sp. strain PCC6803 and their interaction with the membrane. Biochim Biophys Acta 1787:272–279

Bittersmann E, Vermaas W (1991) Fluorescence lifetime studies of cyanobacterial photosystem II mutants. Biochim Biophys Acta 1098:105–116

Bruce D, Brimble S, Bryant DA (1989) State transitions in a phycobilisome-less mutant of the cyanobacterium *Synechococcus* sp. PCC 7002. Biochim Biophys Acta 974:66–73

Gantt E (1981) Phycobilisomes. Annu Rev Plant Physiol 32:327–347

Gardian Z, Bumba L, Schrofel A, Herbstova M, Nebesarova J, Vacha F (2007) Organisation of photosystem I and photosystem II in red alga *Cyanidium caldarium*: encounter of cyanobacterial and higher plant concepts. Biochim Biophys Acta 1767:725–731

Glazer AN (1984) Phycobilisome: a macromolecular complex optimized for light energy-transfer. Biochim Biophys Acta 768:29–51

Kruip J, Bald D, Boekema E, Rögner M (1994) Evidence for the existence of trimeric and monomeric photosystem I complexes in thylakoid membranes from cyanobacteria. Photosynth Res 40:279–286

Ley AC, Butler WL (1977) Energy transfer from photosystem II to photosystem I in *Porphyridium cruentum*. Biochim Biophys Acta 462:290–294

Liu H, Zhang H, Niedzwiedzki DM, Prado M, He G, Gross ML, Blankenship RE (2013) Phycobilisomes supply excitations to both photosystems in a megacomplex in cyanobacteria. Science 342:1104–1107

McConnell MD, Koop R, Vasil'ev S, Bruce D (2002) Regulation of the distribution of chlorophyll and phycobilin-absorbed excitation energy in cyanobacteria. A structure-based model for the light state transition. Plant Physiol 130:1201–1212

Mimuro M, Yamazaki I, Tamai N, Katoh T (1989) Excitation energy transfer in phycobilisomes at −196 °C isolated from the cyanobacterium *Anabaena variabilis* (M-3): evidence for the plural transfer pathways to the terminal emitters. Biochim Biophys Acta 973:153–162

Mimuro M, Akimoto S, Tomo T, Yokono M, Miyashita H, Tsuchiya T (2007) Delayed fluorescence observed in the nanosecond time region at 77 K originates directly from the photosystem II reaction center. Biochim Biophys Acta 1767:327–334

Mimuro M, Yokono M, Akimoto S (2010) Variations in photosystem I properties in the primordial cyanobacterium *Gloeobacter violaceus* PCC 7421. Photochem Photobiol 86:62–69

Mörschel E, Schatz GH (1987) Correlation of Photosystem 2 complexes with exoplasmatic freeze-fracture particles of thylakoids of the cyanobacterium *Synechococcus* sp. Planta 172:145–154

Mullineaux CW (2008) Phycobilisome-reaction centre interaction in cyanobacteria. Photosynth Res 95:175–182

Mullineaux CW, Tobin MJ, Jones GR (1997) Mobility of photosynthetic complexes in thylakoid membranes. Nature 390:421–424

Murata N (1969) Control of excitation transfer in photosynthesis. I. Light-induced change of chlorophyll a fluorescence in *Porphyridium cruentum*. Biochim Biophys Acta 172:242–251

Murata N, Satoh K (1986) Absorption and fluorescence emission by intact cells, chloroplasts, and chlorophyll–protein complexes. In: Govindjee, Amesz J, Fork DC (eds) Light emission by plants and bacteria. Academic Press, Orlando, pp 137–159

Niwa K, Kikuchi N, Iwabuchi M, Aruga Y (2004) Morphological and AFLP varation of *Porphyra yezoensis* Ueda form. *narawaensis* Miura (Bangiales, Rhodophyta). Phycol Res 41:294–304

Niwa K, Hayashi Y, Abe T, Aruga Y (2009) Induction and isolation of pigmentation mutants of *Porphyra yezoensis* (Bangiales, Rhodophyta) by heavy-ion beam irradiation. Phycol Res 57:194–202

Olive J, Ajlani G, Astier C, Recouvreur M, Vernotte C (1997) Ultrastructure and light adaptation of phycobilisome mutants of *Synechocystis* PCC 6803. Biochim Biophys Acta 1319:275–282

Shimada Y, Tsuchiya T, Akimoto S, Tomo T, Fukuya M, Tanaka K, Mimuro M (2008) Spectral properties of the CP43-deletion mutant of *Synechocystis sp*. PCC 6803. Photosynth Res 98:303–314

Shubin VV, Tsuprun VL, Bezsmertnaya IN, Karapetyan NV (1993) Trimeric forms of the photosystem I reaction center complex pre-exist in the membranes of the cyanobacterium *Spirulina platensis*. FEBS Lett 334:79–82

Tomo T, Shinoda T, Chen M, Allakhverdiev SI, Akimoto S (2014) Energy transfer processes in chlorophyll *f*-containing cyanobacteria using time-resolved fluorescence spectroscopy on intact cells. Biochim Biophys Acta 1837:1484–1489

Ueno Y, Aikawa S, Kondo A, Akimoto S (2015) Light adaptation of the unicellular red alga *Cyanidioschyzon merolae*, probed by time-resolved fluorescence spectroscopy. Photosynth Res 125:211–218

Ueno Y, Aikawa S, Kondo A, Akimoto S (2016) Energy transfer in cyanobacteria and red algae: confirmation of spillover in intact megacomplexes of phycobilisome and both photosystems. J Phys Chem Lett 7:3567–3571

Yokono M, Murakami A, Akimoto S (2011) Excitation energy transfer between photosystem II and photosystem I in red algae: larger amounts of phycobilisome enhance spillover. Biochim Biophys Acta 1807:847–853

Yokono M, Tomo T, Nagao R, Ito H, Tanaka A, Akimoto S (2012) Alterations in photosynthetic pigments and amino acid composition of D1 protein change energy distribution in photosystem II. Biochim Biophys Acta 1817:754–759

Yokono M, Takabayashi A, Akimoto S, Tanaka A (2015a) A megacomplex composed of both photosystem reaction centres in higher plants. Nat Commun 6:6675

Yokono M, Nagao R, Tomo T, Akimoto S (2015b) Regulation of excitation energy transfer in diatom PSII dimer: how does it change the destination of excitation energy? Biochim Biophys Acta 1847:1274–1282